

Sliding Wear Behavior of Cast Iron: Influence of MoS₂ and Graphite Addition to the Oil Lubricant

B.K. Prasad, S. Rathod, M.S. Yadav, and O.P. Modi

(Submitted September 12, 2009; in revised form March 11, 2010)

The present study discusses sliding wear characteristics of a gray cast iron over a range of applied loads in oil lubricated condition. Effects of MoS₂ and graphite addition to the oil lubricant in governing the wear behavior have also been studied. The wear rate increased with load in general with a few exceptions in the case of oil plus 5% MoS₂ wherein it had a tendency to show a reverse trend in the intermediate load range. Addition of 5% graphite to the oil brought about a decrease in the wear rate without affecting seizure resistance. Increasing quantity of graphite in the oil from 5 to 10% practically did not affect the wear rate at lower loads. However, it led to significantly lower wear rates at higher loads and also offered higher seizure resistance. In the case of oil plus 5% MoS₂ lubricant mixture, the wear rate of the samples was higher than that of the lubricant with 5% graphite when tests were conducted at lower loads while identical response was observed at higher loads in both cases. Seizure resistance of the samples was not affected by the addition of 5% graphite and MoS₂ to the oil. The frictional heating also increased with load in general, except in the case of oil containing 5% MoS₂ and 10% graphite wherein it remained practically unaffected in the intermediate load range. The presence of 5% graphite and MoS₂ in the oil lubricant brought about reduced frictional heating, except in the case of oil plus 5% graphite mixture wherein the trend reversed, and oil plus 5% MoS₂ leading to comparable frictional heating during specimen seizure. Increasing test duration caused higher frictional heating. Adhesion was observed to be the principal wear mechanism while microcracking assisted delamination and abrasion also contributed to material loss.

Keywords cast iron, graphite, MoS₂, oil, sliding wear, solid lubricant

1. Introduction

Cast iron has been in use as tribocomponents in several engineering applications (Ref 1-3). Many of the applications involve sliding in the presence of lubricants. There exist several types of lubricants, oil being one of the most popular ones used in practice. It contains a variety of additives including solid lubricants with a view to realize improved performance (Ref 4-28). The recent trend in this context has been to add nano-size particles of metals like Al, Sn, and Ni as well as those of WS₂ to the oil lubricants (Ref 15-17). Some studies also refer to the addition of graphite and MoS₂ particles as a suspension in the oil in this direction (Ref 4, 8-10, 13, 14, 18, 19, 21, 23-28). The two solid lubricants possess very low hardness (1-2 Mohs) and favorable crystal structure (Ref 4-7, 29-33), (<http://www.dynamiccoatingsinc/mdy.htm>). Further, graphite stands much lighter and cheaper than that of MoS₂.

It may be mentioned that graphite possesses an open hexagonal layered structure with the ratio of interplanar to interatomic distances as 2.403 that is much higher than that of an ideal hexagonal close packed structure (Ref 5, 29, 34). This

makes the bonds between the parallel layers, i.e., basal planes, relatively weaker (van der Waals type) in contrast with covalent bonds in the basal plane (Ref 5). The ability of graphite to form strong chemical bonds with gases and water vapor adsorbed onto the crystalline edges further adds to the solid lubricating capability of graphite since the adsorbed mass further weakens the interlayer bonding resulting in the easy shear and transfer of the crystalline platelets of the material onto the mating surfaces (Ref 5, 31, 32). MoS₂ also has a layered structure like graphite (Ref 30, 35, 36). Because of the weak van der Waals interaction between the sheets of sulfide atoms, MoS₂ acts as a solid lubricant (Ref 30). In its appearance and feel, MoS₂ is similar to graphite and indeed it is widely used as a solid lubricant because of its low friction properties, sometimes at relatively higher temperatures (Ref 30).

Studies have shown that the influence of solid lubricant additives on the performance of oil lubricants is controlled by factors like the nature and characteristics of the solid and base lubricants as well as that of sliding pair and conditions (Ref 8, 9). The content and mode of their incorporation and distribution into the sliding material system and base lubricant also has an important bearing on their overall response during sliding. A solid lubricant could be used either by mixing with the base (oil/grease) lubricant (Ref 4, 8-11, 13-20) or through its dispersion in the sliding material system (Ref 37-39). Soft nature (hardness level 1-2 Mohs) of the solid lubricants adversely affects the relevant mechanical properties like strength of the matrix material system (Ref 40). Also, cracking tendency imparted by the (mechanically) dispersed solid lubricant particles also makes the material system crack sensitive thereby adversely affecting the sliding wear response under the condition of its predominance (Ref 41-45).

B.K. Prasad, S. Rathod, M.S. Yadav, and O.P. Modi, Advanced Materials and Processes Research Institute (CSIR), Bhopal 462064, India. Contact e-mail: braj_kprasad@yahoo.co.in.

Accordingly, beneficial effects of solid lubricants could be realized in very specific cases only in the case of materials containing dispersed solid lubricant particles (Ref 41-45). This limitation could be taken care of to a great extent by mixing the solid lubricant phase with the base (oil/grease) lubricant wherein the lubricant particles get a better opportunity to reach the contacting surfaces and smear producing lubrication effect more effectively.

Sliding wear behavior of cast iron has been studied over the past investigating the effects of material microstructure, applied load/pressure, sliding speed, and test environment on the wear response (Ref 9, 10, 12, 23-28, 46-54). Some of them also refer to the effect of adding solid lubricant particles in oil on the wear behavior of cast iron (Ref 9, 11, 12, 23-28). Parameters studied therein include quantity and type of the solid lubricant, sliding material (cast iron) type and microstructure, sliding speed, and load/pressure (Ref 9, 11, 12, 23-28). The studies suggest that the mentioned parameters have a strong bearing on the overall wear performance of the material system (Ref 9, 11, 12, 23-28). However, information pertaining to the direct comparison of the relative performance of graphite vis-a-vis MoS₂, when mixed in oil lubricant, in terms of controlling the sliding wear response of cast irons does not exist to the best of our knowledge. Further, since the wear response of materials depends on a number of material and test (operating) parameters and a synergistic effect on wear behavior is produced by such factors, examination of wear performance of materials on a case-to-case basis gives a more realistic picture.

In view of the above, an attempt has been made in this study to investigate the effect of adding graphite and MoS₂ particles on the lubrication capability of an oil lubricant toward controlling the wear response of a gray cast iron over a range of applied loads. The observed wear behavior has been discussed in terms of specific features of various microconstituents of the samples and substantiated through the features of wear surfaces, subsurface regions, and debris particles.

2. Experimental

2.1 Material and Specimen Preparation

The cast iron (Table 1) was prepared in the form of 20-mm diameter and 150-mm long cylindrical castings. Specimens for microstructural and wear property characterization were prepared from the castings. The samples for microstructural studies were in the form of 20-mm diameter and 15-mm thick discs. They were polished metallographically and etched with 2% nital solution prior to their microstructural examination. The samples for wear property characterization were prepared in the form of 8-mm diameter and 53-mm long cylindrical pins. They

also comprised of a 1.5-mm diameter hole drilled at a distance of 1.5-mm from the contacting surface. The pin and the disc were polished up to a roughness (Ra) level of 0.82 μm and cleaned well with acetone and carbon tetrachloride prior to and after wear testing. The specimens for wear surface and subsurface studies were prepared from the wear tested samples. The samples for wear surface examination were cleaned well, mounted on brass studs and sputtered with gold prior to their examination. The specimens for subsurface characterization were cut as longitudinal sections normal to the wear surface in the direction of sliding. They were mounted in polyester resin, polished as per standard metallographic techniques and etched with 2% nital solution prior to mounting on the brass studs and gold sputtering. The debris was cleaned with carbon tetrachloride and acetone. It was spread on a glass slide and fixed on brass studs with the help of a double sided tape prior to gold sputtering.

2.2 Sliding Wear Tests

Sliding wear tests were performed using a Cameron-Plint make pin-on-disc machine at a sliding speed of 4.2 m/s over a range of applied loads for a predetermined sliding distance of 2500 m or prior to seizure. The applied load on the specimens was increased in steps from 50 N (corresponding to 1 MPa pressure for the 8-mm diameter pin sample) to until specimen seizure prior to negotiating the specified sliding distance. A schematic representation of the test configuration is shown in Fig. 1. The disc was fabricated using En25 (corresponding to AISI 4340) steel. Table 1 show the nominal chemical composition and hardness of the disc. The track diameter used was 80 mm. The load on the samples was applied using

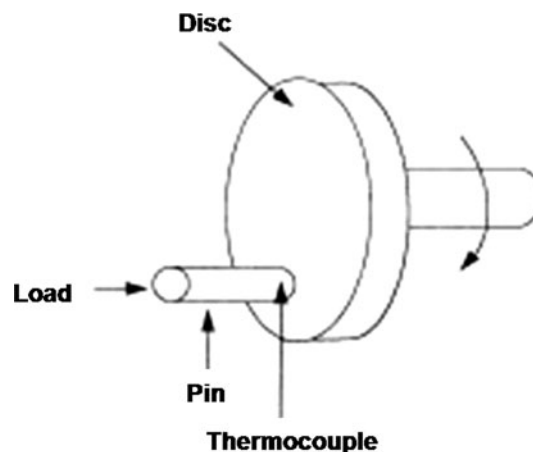


Fig. 1 A schematic representation of the wear test configuration

Table 1 Chemical composition and hardness of the experimental pin and disc materials

| Material | Chemical composition, element (wt.%) | | | | | | | Hardness, HV |
|-------------------|--------------------------------------|------|------|------|------|------|------|--------------|
| | Fe | Si | C | Mn | Ni | Cr | Mo | |
| Cast Iron (Pin) | ^a | 2.58 | 3.25 | 0.49 | ... | ... | ... | 220 |
| EN25 Steel (Disc) | ^a | 0.23 | 0.30 | 0.58 | 2.50 | 0.70 | 0.50 | 318 |

^aRemainder

a hydraulically operated loading mechanism. The temperature near the specimen surface was monitored during the tests by inserting a chromel-alumel thermocouple in the hole made near the contacting surface. The cleaned pin samples were weighed prior to and after the wear tests using a Mettler microbalance with a precision level of 0.01 mg. Wear rate was computed by weight loss technique and an average of three observations considered. The lubricant mixture was prepared by thoroughly mixing (severe hand stirring using a glass rod) graphite or MoS₂ particles in SAE 40 oil. The viscosity of the oil was 319 centipoise. The particle size range of graphite was 10-100 μm while that of MoS₂ 1-20 μm. Figure 2 show the solid lubricant (graphite and MoS₂) particles. Layered structure was observed in the case of graphite (Fig. 2b, c) as well as MoS₂ (Fig. 2e). The concentration of graphite was varied in the range of 5-10 wt.% while that of MoS₂ was fixed at 5 wt.% in a bid to maintain homogeneity of distribution of the suspended particles

in the lubricant mixture. The mentioned range of concentration of graphite selected in this study was based on earlier studies suggesting it to offer the best wear response (Ref 12, 24).

The test procedure involved immersing the polished and cleaned disc in the lubricant mixture and rotating the lubricated disc at a speed of 2.68 m/s for 5 s in order to make the thickness of the lubricant uniform on the disc surface and maintain condition close to mixed lubrication where both elastohydrodynamic and boundary lubricated regions within a single contact are suggested to exist (Ref 17). This was followed by loading the polished and cleaned specimen against the lubricated disc with the help of a hydraulically operated loading mechanism and allowing the disc to rotate for a predetermined distance of 2500 m or until specimen seizure. Load on the samples was increased in steps until the occurrence of specimen seizure prior to traversing the predetermined sliding distance. Seizure was monitored in terms of substantial

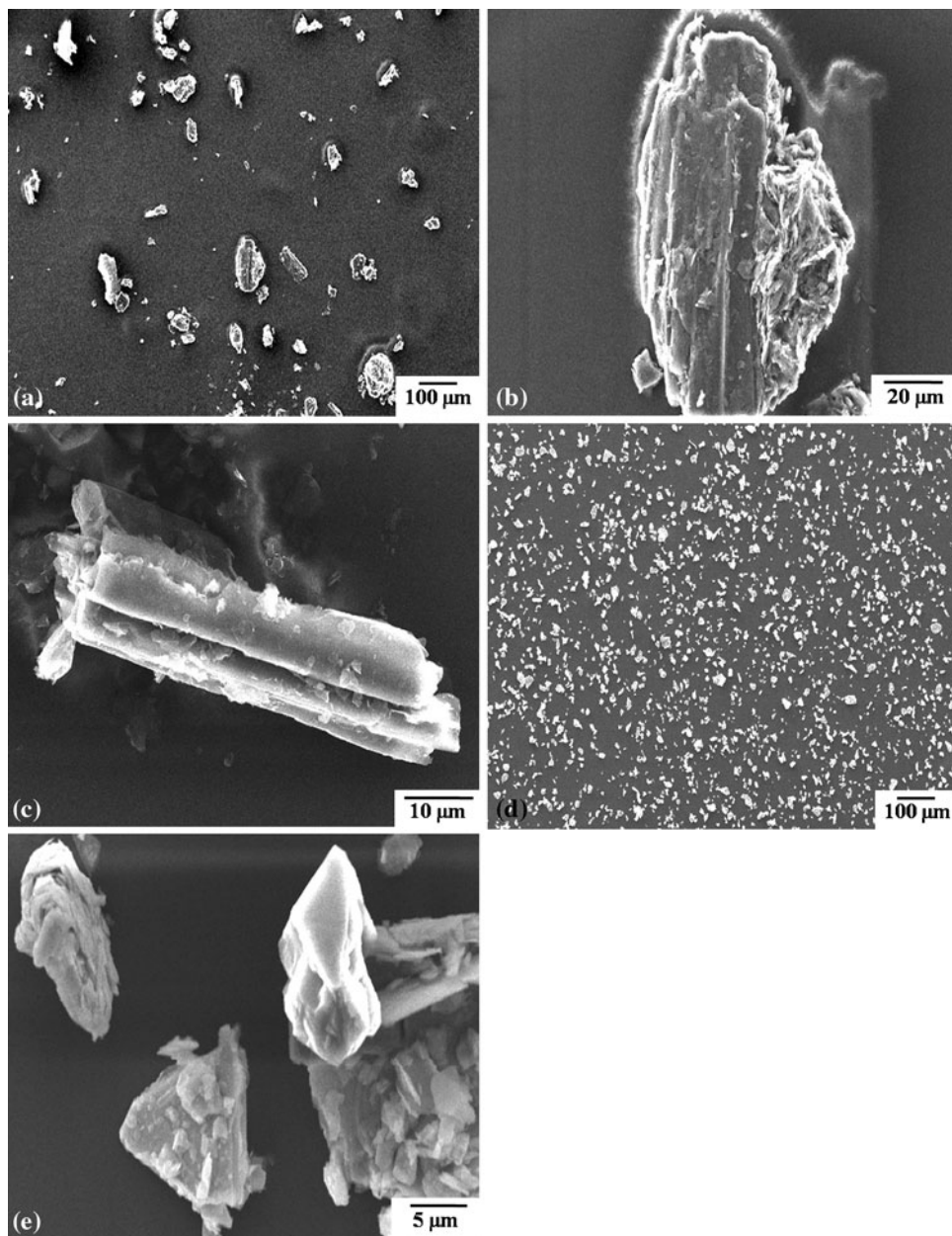


Fig. 2 Micrographs of (a-c) graphite and (d, e) MoS₂ powder particles used as the solid lubricant in the oil lubricant mixture

adhesion of the specimen material onto the disc, burning of the lubricant and abnormal noise in the pin-disc assembly.

2.3 Microscopy and Microstructure

Microstructural characterization of the samples was carried out on metallographically polished and etched samples using optical and scanning electron microscopes. The wear surfaces, subsurface regions, and debris particles were studied with the help of a scanning electron microscope (SEM). The SEM was JEOL make JSM5600 while the optical microscope was Leitz make. Figure 3 show the microstructure of the cast iron. Different microconstituents observed were pearlite, (free) ferrite and graphite.

3. Results

3.1 Wear Behavior

Figure 4 show the wear rate of the samples plotted as a function of applied load. The effects of adding MoS₂ and graphite to the oil on the wear rate are also evident from the figure. The wear rate increased with load in general except in some cases wherein a reverse trend was noted in the intermediate range of load. The wear rate versus load plots revealed three slopes in general. The slope was high in the low and high load ranges while a mixed trend was noticed in the intermediate range of load. Addition of 5% solid lubricant particles to the oil lubricant led to lower wear rate. The wear performance of the samples in the oil lubricant containing 5% MoS₂ was somewhat inferior to the one with 5% graphite especially at lower loads, while it became comparable in the higher load range. Further, increasing the graphite content of the oil from 5 to 10% did not affect the wear rate at lower loads. However, this exercise led to significantly lower wear rates at higher loads and also offered higher seizure resistance.

Figure 5 show temperature near the specimen surface as a function of test duration. The severity of frictional heating

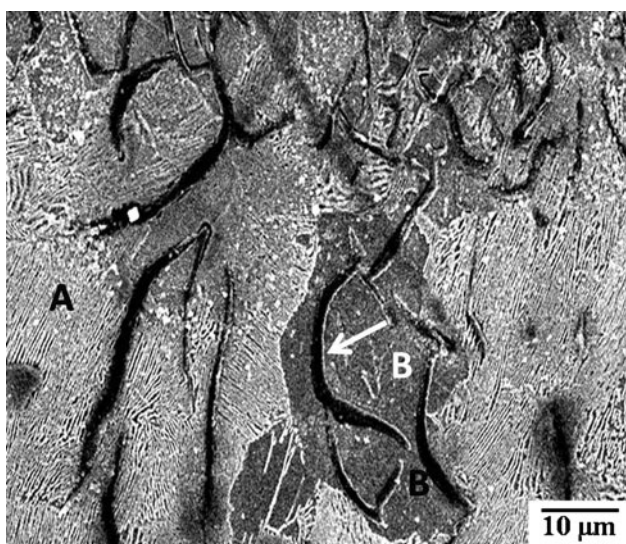


Fig. 3 Microstructural features of the samples showing various microconstituents [A: pearlite, B: ferrite, and single arrow: graphite]

increased with the test duration. The rate of temperature increase was high initially. This was followed by a reduction in the rate of frictional heating at longer test durations. In some cases, especially at high loads, the slope became high once again toward the end of the test (Fig. 5d). The frictional heating increased with load while the test environment produced a mixed effect.

The maximum temperature near the specimen surface has been plotted as a function of applied load in Fig. 6. The severity of frictional heating increased with load while the presence of MoS₂ and graphite particles in the oil lubricant caused the severity of temperature increase to reduce in general. Further, the changing concentration of graphite produced a mixed influence on temperature.

3.2 Wear Surfaces

Wear surfaces of the samples tested in the oil plus graphite lubricant mixture are shown in Fig. 7. The wear surfaces were smooth in general at low loads (Fig. 7a). Deep grooves were also observed (Fig. 7a). A magnified view showed microcracks on the surface (Fig. 7b). The surface damage became more severe as the load was increased (Fig. 7c vs. a). The changing graphite content in the oil lubricant did not affect the trend significantly as far as the effect of load on the nature of wear surface is concerned (Fig. 7f vs. d). Exposure of graphite and its smearing on the sliding surface were noted (Fig. 7e). Microcracks may be seen in Fig. 7g.

Figure 8 show the wear surfaces of the samples tested in the oil plus MoS₂ lubricant mixture. The severity of surface damage increased with load (Fig. 8d vs. a). Entrapment of the solid lubricant phase (Fig. 8b) and its flow in the sliding direction may be seen in Fig. 8c. Presence of deep grooves, dark patches and smearing of the lubricant phase were also observed (Fig. 8c-e, respectively).

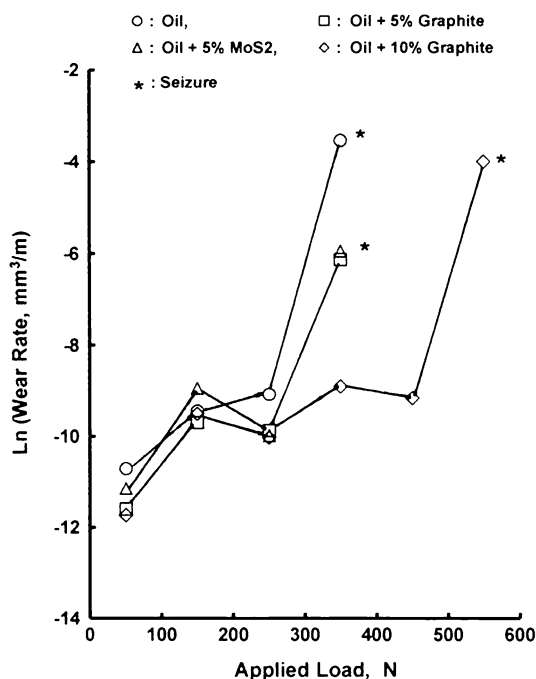


Fig. 4 Wear rate versus applied load plots of the samples tested in different environments

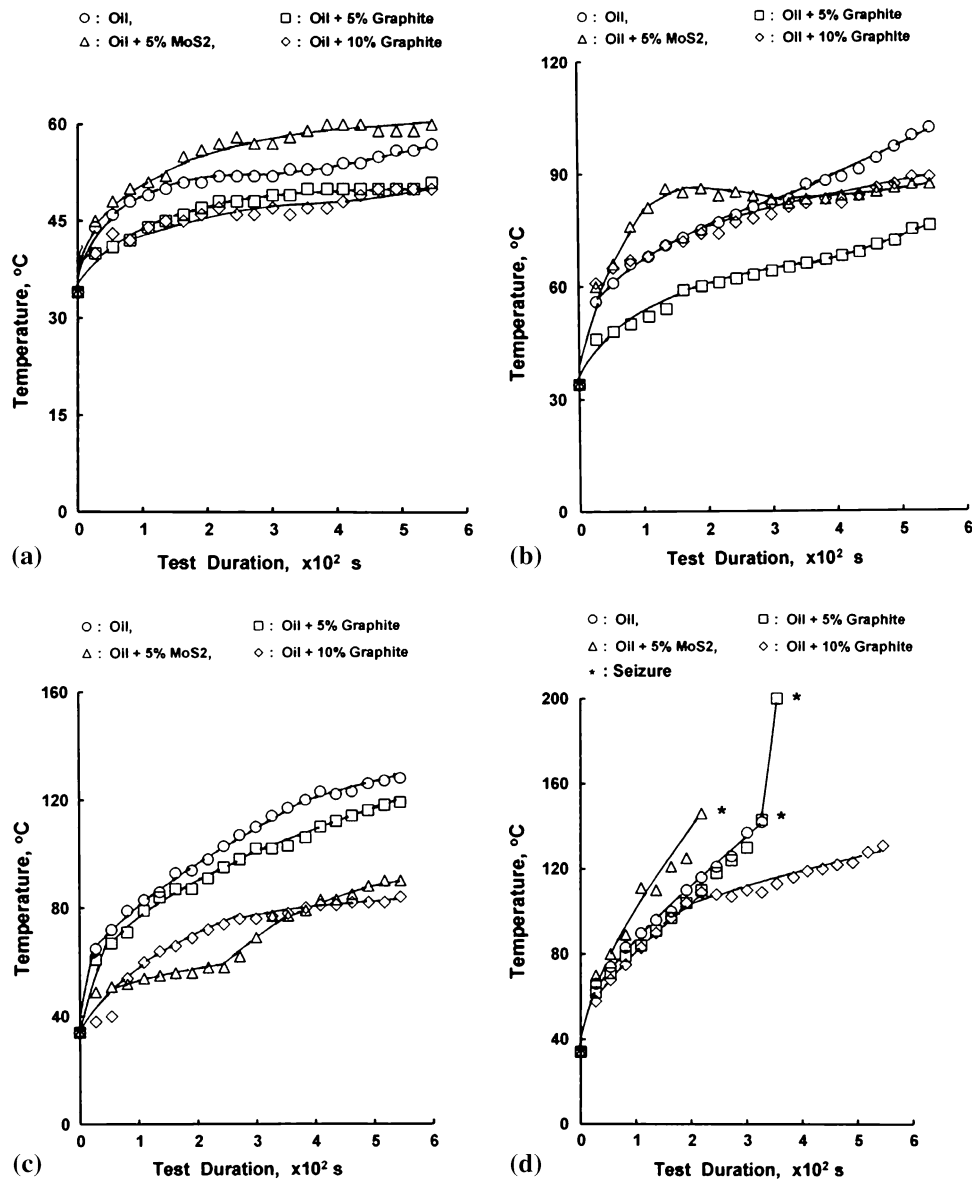


Fig. 5 Temperature near the specimen surface vs. test duration plots tested at (a-d) different environments at (a) 50 N, (b) 150 N, (c) 250 N, and (d) 350 N loads

3.3 Subsurface Regions

Figure 9 show subsurface regions of the samples. Figure 9(a) show a typical example of a practically undeformed region in a process of being separated from the bulk at low applied pressures. A magnified view show the presence of microcracks (Fig. 9b). Broadly speaking, the degree of deformation decreased with increasing depth below the wear surface. The topmost region undergoing most severe deformation comprised of finest microconstituents (Fig. 9e, f). This was followed by the presence of flow of microconstituents in the sliding direction and unaffected bulk structure (Fig. 9a-d).

3.4 Wear Debris

Figure 10 show the debris particles. The debris comprised of deformed flakes in general (Fig. 10a, d). The region marked by single arrow in Fig. 10a showed layered structure (Fig. 10b).

Machining chips and particles with sharp tips and edges were also noticed in the debris (Fig. 10c, d, respectively).

4. Discussion

The wear response of materials is greatly controlled by the specific nature of their various microconstituents and predominance of one set of parameters bringing about improved wear behavior over the other leading to an opposite influence. As far as the cast iron studied in this investigation is concerned, ferrite being soft and ductile (Ref 34) provides compatibility to the weak and poorly wettable graphite flakes and hard pearlite (Ref 41-45). The sharp tips and edges of cementite within pearlite provide potential sites for the nucleation and propagation of microcracks while pearlite as a whole being hard and

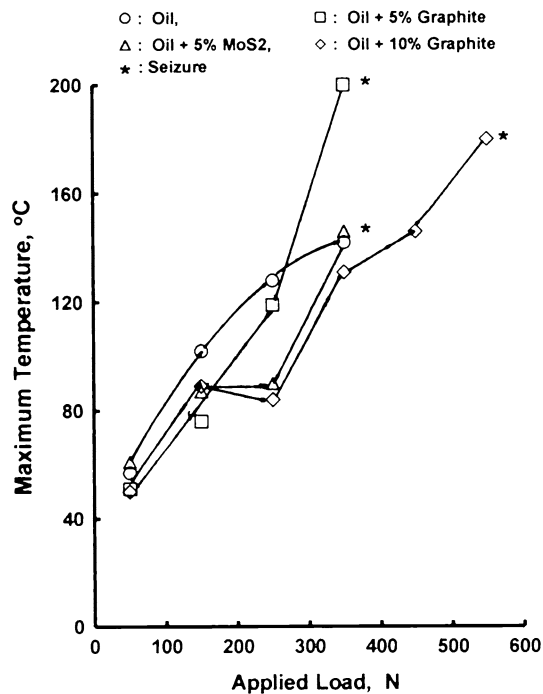


Fig. 6 Maximum temperature near the specimen surface vs. applied load plots for the cast iron tested in different environments

strong imparts load bearing capability to the material system (Ref 11, 55). Graphite in the cast iron is the softest among all the microconstituents and, from strength point of view, behaves as porosity thereby causing weakening of the material (Ref 40, 41). Also, due to negligible solid solubility, graphite exists as a mechanical mixture (Ref 40-45) despite its precipitation from within the melt (matrix). Accordingly, graphite/matrix interface acts as a potential site for the nucleation and propagation of cracks (Ref 40). However, graphite provides solid lubrication through smearing and forming lubricant film on the contacting surfaces under optimized sliding conditions (Ref 38-45). The presence of an external lubricant like oil suppresses the cracking tendency of the material and allows more effective formation of lubricant films (Ref 8, 9, 12). The graphite in the cast iron also gets a better opportunity to smear and form a solid lubricant film. The triboinduced reaction products such as self-generated oxide films form during sliding that increase the resistance of the contacting asperities against crumbling (Ref 56). The external (oil) lubricant also imparts good wettability to the solid lubricant films formed. The presence of a solid lubricant phase in the oil lubricant enables to realize more effective formation of lubricant films that have greater stability and cover a wider portion of the sliding surfaces leading to improved wear behavior. This continues up to a critical content of the solid lubricant in the oil (Ref 8, 9, 12). Solid lubricant particles in quantities higher than the optimum make the lubricant mixture inhomogeneous in view of segregation of the suspended mass; higher the density of the solid lubricant, greater the degree of segregation in the lubricant mixture. The segregation renders the film too dry and too thick to stick effectively onto the contacting surfaces resulting into its peeling off and thus adversely affecting wear response (Ref 8, 12).

Reduced wear rate of the samples at lower loads (Fig. 4) could be substantiated through smoother and less damaged wear surfaces (Fig. 7a vs. c, 7d vs. f, and 8a vs. d) and less

frictional heating (Fig. 5, 6). A decrease in the slope of the wear rate versus load plots in the intermediate range of loads (Fig. 4) could be due to the more effective formation and greater stability of the triboinduced lubricant film. On the contrary, very high slope during specimen seizure results from mass adhesion of the fused material onto the disc surface in view of high frictional heat generated due to severe wear condition (Ref 45). Somewhat inferior (at lower loads) or comparable (at higher loads) wear performance of the samples in the oil containing 5% MoS₂ to that of the one with 5% graphite was observed. This was despite the fact that MoS₂ is a more effective solid lubricant than that of graphite (Ref 30). The reason to this could be the fact that factors controlling the wear performance of the solid lubricants include particle size and density apart from their intrinsic chemical and structural characteristics. Higher density (5.06 g/cc) of MoS₂ than that of graphite (2.09-2.23 g/cc) (Ref 30) suggests (a) greater possibility of MoS₂ getting more of its particles thrown out of the rotating disc surface due to centrifugal force during sliding, thus leaving less of the compound left on the contacting surfaces to smear and produce solid lubricating effect, (b) less effective volume fraction in the oil lubricant mixture thereby covering less area for forming solid lubricant film on the sliding surfaces, and (c) greater tendency toward segregation in the oil lubricant mixture. The mentioned factors arising out of higher density adversely affect the performance of MoS₂. However, the finer particle size of MoS₂ (1-20 μm) than that of graphite (10-100 μm), as also evident from Fig. 2, suggests more surface area of the MoS₂ particles available for establishing contact with the sliding surfaces. Under the circumstances, their smearing and subsequently lubricant film formation becomes more effective thus leading to improved performance. The adverse effects of higher density of MoS₂ on its solid lubricating characteristics seem to dominate the positive influence of its finer particle size making it to perform comparable to the lighter and coarser graphite in this study despite the reported better lubricating characteristics of MoS₂ as compared to that of graphite (Ref 30).

High rate of frictional heating with increasing test duration in the beginning of the tests (Fig. 5) could be attributed to the abrasion caused by the fragmentation and work hardening of the initially contacting asperities that constitute only a minor fraction of the apparent area of the contacting surfaces (Ref 57-59). This makes them to carry the entire applied load that far exceeds their yield stress and makes them to yield, fragment and work harden in the due course of sliding (Ref 59). Fragmentation of the initially contacting asperities increases the number of subsequently contacting asperities thereby making the wear condition mild. This finally leads to a reduced rate of temperature increase at longer test durations (Fig. 5). A further increase in the rate of frictional heating toward the end of the tests in some cases could be attributed to the destabilization of the lubricant film.

Smearing and flow of the solid lubricant phase (Fig. 7e, 8c-e), presence of dark patches on the wear surfaces (Fig. 7d, 8d) and flow of graphite in the sliding direction in the subsurface regions (Fig. 9b-d) suggest the formation of lubricant film during sliding. Further, the flow of microconstituents and the presence of plastically deformed regions on the wear surface (Fig. 7d, f, 8c, d) as well as in the subsurface regions (Fig. 9), and deformed flakes in the wear debris (Fig. 10a, d) indicate adhesion to be the dominant wear mechanism. On the contrary, the presence of microcracks on the wear surfaces (Fig. 7b, g)

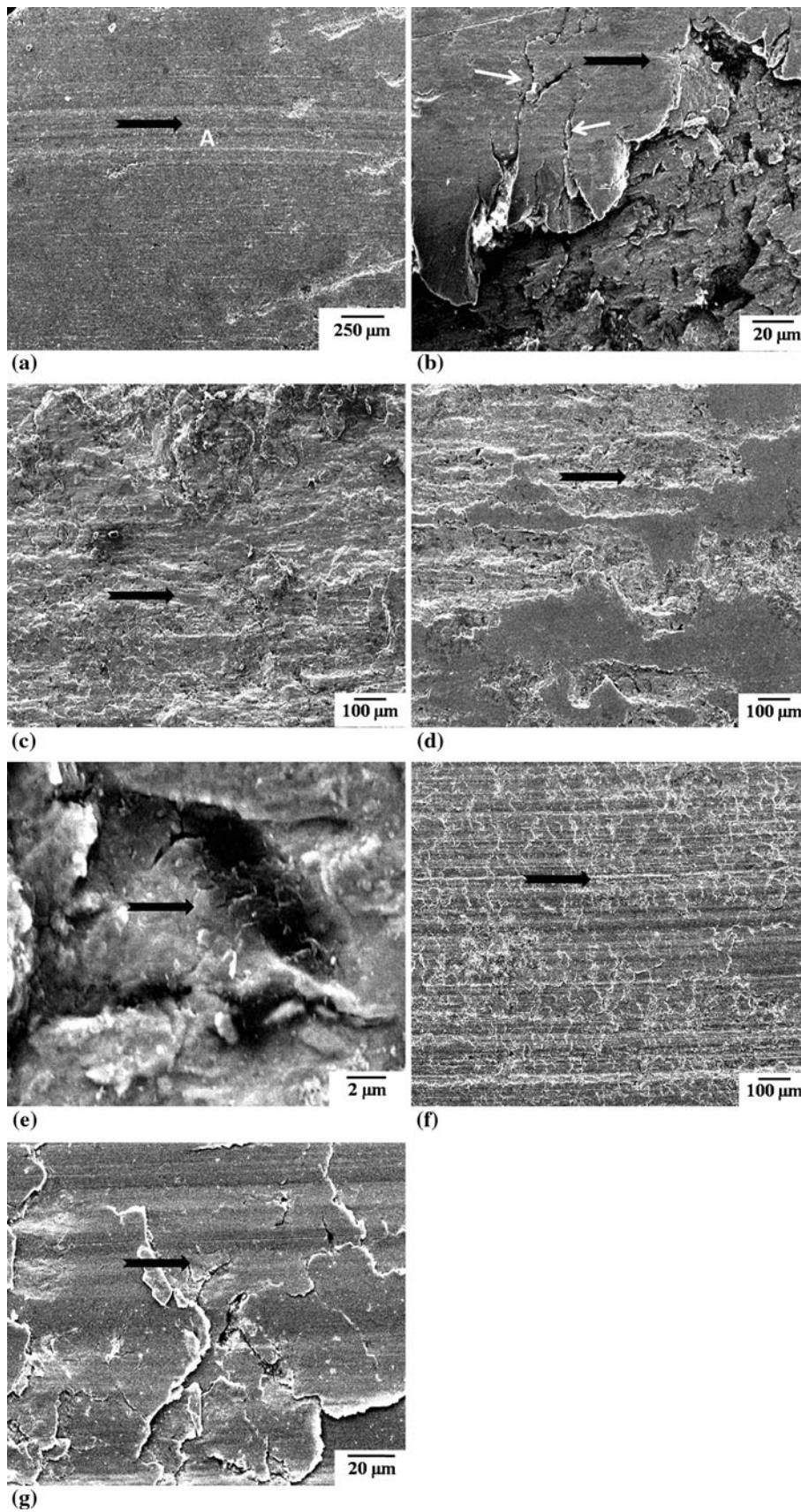


Fig. 7 Wear surfaces of the samples tested in the oil lubricant mixture containing (a-c) 10% graphite and (d-g) 5% graphite at the applied load of (a, b) 50 N, (c) 550 N, (d, e) 250 N, and (f, g) 350 N. \rightarrow indicates the sliding direction [A: deep grooves and arrow: microcracks]

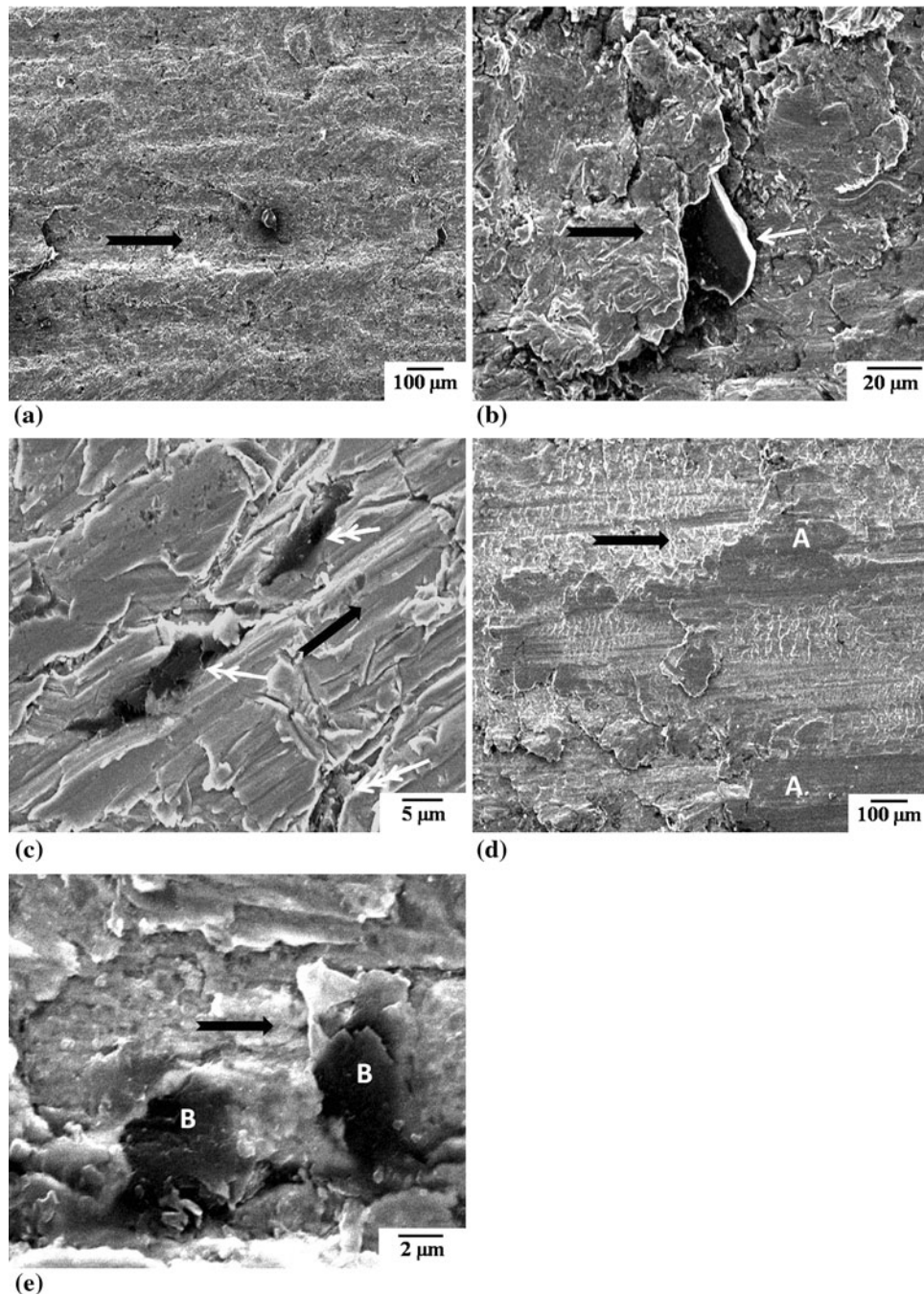


Fig. 8 Wear surfaces of the samples tested in the oil lubricant mixture containing 5% MoS₂ particles at the applied load of (a-c) 50 N and (d-e) 350 N. → indicates the sliding direction [Single arrow: entrapped solid lubricant particle, double arrow: flow of graphite flake in the sliding direction, triple arrow: deep grooves, A: dark patches and B: smearing of the solid lubricant (graphite/MoS₂) phase]

and below the contacting surfaces (Fig. 9b) indicates delamination also to contribute to material loss. Deep grooves on the wear surfaces (Fig. 7a) are caused by the abrasive action of machining chips (Fig. 10c) and other hard microconstituents of the sliding pair that get entrapped in between the contacting surfaces (Ref 41-45, 57). They suggest abrasion also to play a role in causing material removal. The layered particles (Fig. 10b) and the ones with sharp edges (Fig. 10d) are the solid lubricant phase suspended in the oil lubricant mixture. They get removed from the contacting surfaces due to the centrifugal force experienced during sliding. Their features

(Fig. 10b, d) identical to those of the ones in Fig. 2 further strengthen the view.

Changing microstructural features of the regions below the wear surfaces (Fig. 9) correspond to the varying severity of wear-induced plastic deformation experienced by the regions (Ref 58-61). Highest degree of deformation experienced by the regions in the nearest vicinity of the wear surfaces made them to delineate finest microconstituents (Fig. 9e, f). Factors like high rate of thermal cycling and straining, and high dislocation density have been observed to be responsible for such a microstructural alteration (Ref 62, 63). Decreasing severity of

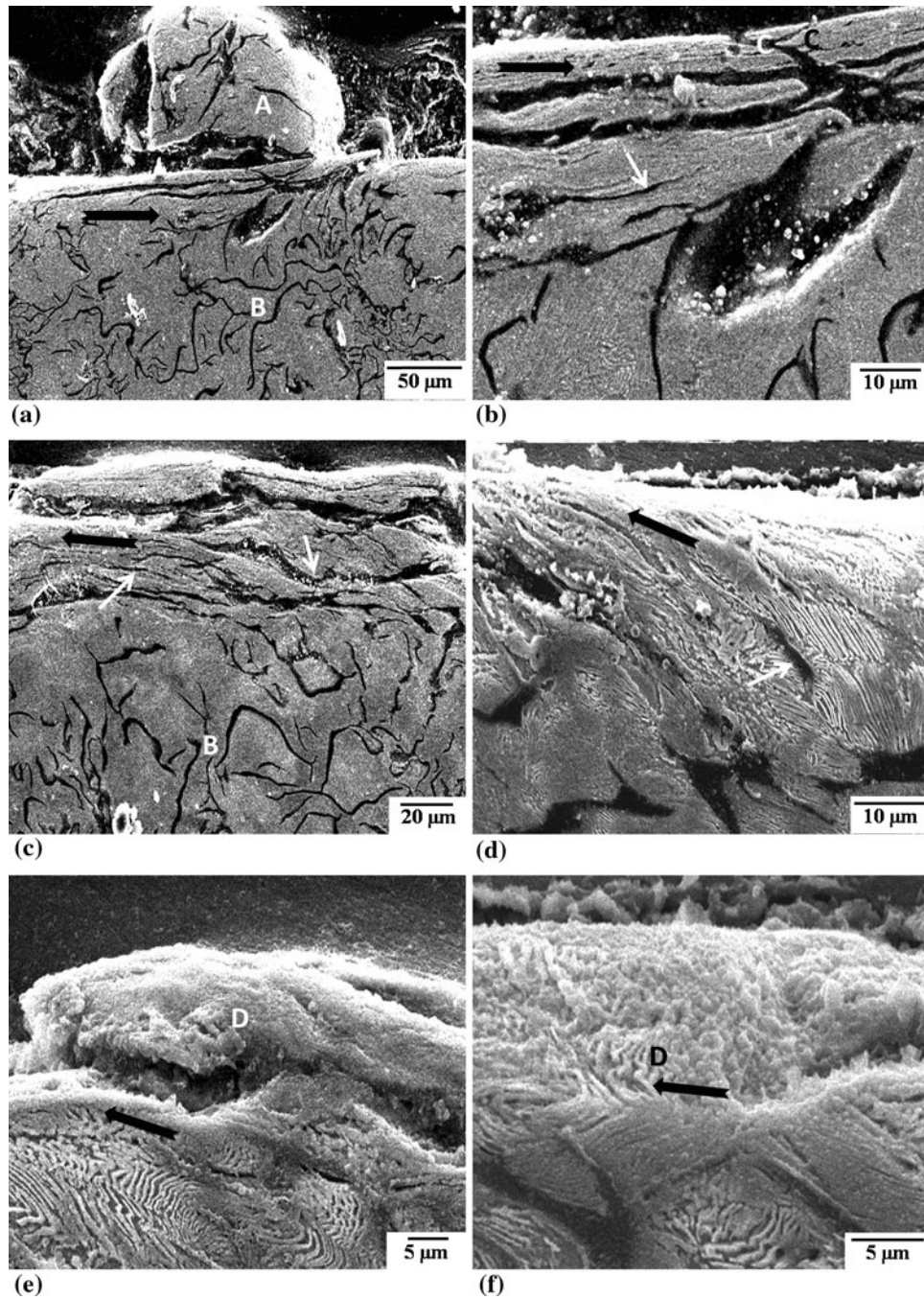


Fig. 9 Subsurface regions of the samples tested in the oil lubricant mixture containing (a-c) 10% graphite and (d-f) 5% MoS₂ particles at the load of (a, b) 50 N, (c) 550 N and (d-f) 350 N. → indicates the sliding direction [A: topmost region revealing negligible plastic deformation, B: bulk structure, C: cracks, single arrow: flow of microconstituent in the sliding direction, and D: heavily deformed structure]

deformation with increasing depth below the wear surface causes the regions next to the topmost one to reveal flow of microconstituents in the sliding direction (Fig. 9c, d) and the ones still below remaining practically unaffected to display features (Fig. 9a, c) identical to those of the bulk (Fig. 3).

5. Conclusions

1. Wear rate of the samples increased with load in general. However, a reverse trend was also noted in the intermediate

load range in some cases. The wear rate versus load plots showed three slopes in general wherein the slope was high in the low and high load ranges while a mixed trend was noticed in the intermediate range of load.

2. Addition of MoS₂ and graphite particles to the oil lubricant led to lower wear rate in general. However, the wear performance of the samples in the oil containing 5% MoS₂ was somewhat inferior to the one with 5% graphite at lower applied loads while it was comparable at higher loads. Also, increasing the graphite content of the oil from 5 to 10% practically did not affect the wear rate at

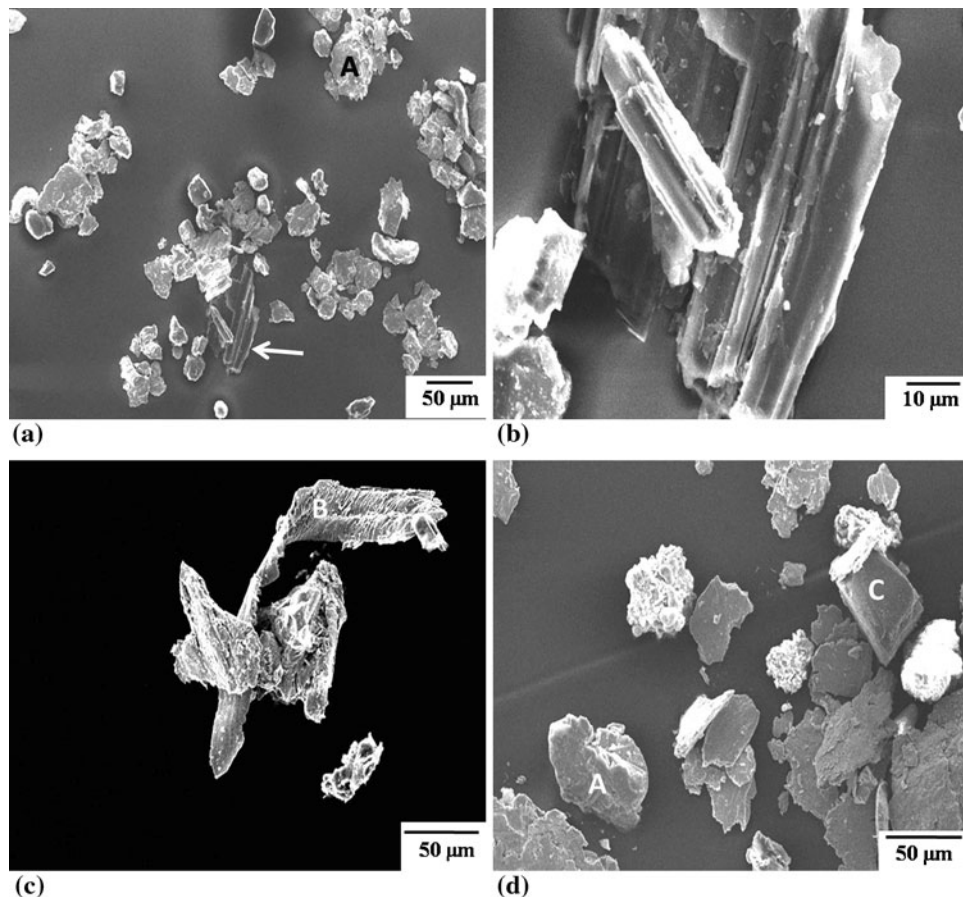


Fig. 10 Debris particles of the samples tested at the applied load of 350 N in the oil lubricant mixture containing 5% (a-c) graphite and (d) MoS₂ particles [Arrow: layered (graphite) particle, A: flake, B: machining chip, and C: fragmented solid lubricant (MoS₂) particle]

lower loads. However, this exercise led to significantly lower wear rates at higher loads and, at the same time, offered higher seizure resistance as well. These observations become significant in the sense that higher graphite contents could be useful in more severe conditions of sliding and that cheaper and lighter graphite could work more effectively than MoS₂ in specific conditions like the ones in this study. Moreover, alteration in the slope of the wear rate plots indicates the changing operating mechanism in typical load regimes. Higher slope corresponds to severe wear regimes while lower slope represents mild wear condition.

3. Temperature near the specimen surface increased with the test duration. The rate of temperature increase was high initially. This was followed by a reduction in the rate of frictional heating at longer test durations. In some cases, especially at high loads, the slope became high once again toward the end of the test. The frictional heating increased with load while the test environment produced a mixed effect. Minimal slope of the wear rate versus pressure plots in the intermediate range of applied pressures indicates the formation of more stable lubricating films on the contacting surfaces to a greater extent.
4. The observed wear response of the samples could be substantiated through the specific features of wear surfaces, subsurface regions, and debris. The latter ones also enabled to understand the operating material removal mechanisms. Adhesion was observed to be the principal

wear mechanism while microcracking assisted delamination and abrasion also contributed to material loss.

References

1. C.V. White, Gray Iron, *Metals Handbook: Properties, Selection: Irons, Steels, High Performance Materials*, Vol. 1, 10th ed., ASM, Materials Park, Ohio, USA, 1990, p 12–32
2. Y. Zhang, Y. Chen, R. He, and B. Shen, Investigation of Tribological Properties of Brake Shoe Materials—Phosphorous Cast Irons with Different Graphite Morphologies, *Wear*, 1993, **166**, p 179–186
3. T.S. Eyre, Friction, Wear of Cast Irons, *Metals Handbook: Friction, Lubrication, Wear Technology*, Vol. 10, 18th ed., ASM, Materials Park, Ohio, USA, 1992, p 695–701
4. M. Yazun, Z. Wancheng, L. Shengna, J. Yuansheng, W. Yusong, and T.C. Simon, Tribological Performance of Three Advanced Piston Rings in the Presence of MoDTC-Modified GF-3 Oils, *Tribol. Lett.*, 2005, **18**, p 75–83
5. F.J. Clauss, Solid Lubricants and Self-Lubricating Solids, Chapter 5, *Handbook of Tribology*, B. Bhushan and B.K. Gupta, Ed., McGraw Hill Inc., USA, 1991, p 5.1–5.86
6. R.H. Boehringer, Grease, *Metals Handbook: Friction, Lubrication, Wear Technology*, Vol. 10, 18th ed., ASM, Materials Park, Ohio, USA, 1992, p 123–131
7. S.Q.A. Rizvi, Lubricant Additives and Their Functions, *Metals Handbook: Friction, Lubrication, Wear Technology*, Vol 10, 18th ed., ASM, Materials Park, Ohio, USA, 1992, p 98–112
8. B.K. Prasad and O.P. Modi, Sliding Wear Response of Zinc-Based Alloy as Affected by Suspended Solid Lubricant Particles in Oil Lubricant, *Tribol. Mater. Surf. Interfaces*, 2008, **2**, p 84–91

9. B.K. Prasad, Lubricated Sliding Wear Behaviour of a Cast Iron: Effect of Graphite and/or Talc Fraction in Oil, *J. Mater. Eng. Perform.*, 2010, **19**, p 413–420
10. F. Wilson and T.S. Eyre, Addition of Graphite Particles to Oil Lubricants, *Lubr. Eng.*, 1973, **29**, p 65–72
11. T.H.C. Childs and F. Sabbagh, Boundary-Lubricated Wear of Cast Irons to Simulate Automotive Piston Ring Wear Rates, *Wear*, 1989, **134**, p 81–97
12. B.K. Prasad, Effectiveness of an Externally Added Solid Lubricant on the Sliding Wear Response of a Zinc–Aluminium Alloy, its Composite and Cast Iron, *Tribol. Lett.*, 2005, **18**, p 135–143
13. J. Gansheimer and R. Holinski, Molybdenum Disulfide in Oils and Greases Under Boundary Lubrication, *Trans. ASME J. Lubr. Technol.*, 1973, **95**, p 242–248
14. B.K. Gupta and B. Bhushan, Fullerene Particles as an Additive to Liquid Lubricants and Greases for Low Friction and Wear, *Lubr. Eng.*, 1994, **50**, p 524–528
15. S. Qiu, Z. Zhou, J. Dong, and G. Chen, Preparation of Ni Nanoparticles and Evaluation of their Tribological Performance as Potential Additives in Oils, *Trans. ASME J. Tribol.*, 2001, **123**, p 441–443
16. G. Liu, X. Li, N. Lu, and R. Fan, Enhancing AW/EP Property of Lubricant Oil by Adding Nano Al/Sn Particles, *Tribol. Lett.*, 2005, **18**, p 85–90
17. L. Rapoport, V. Leshchinsky, I. Lapsker, Yu. Volovik, O. Nepomnyashchy, M. Lvovsky, R. Popovitz-Biro, Y. Feldman, and R. Tenne, Tribological Properties of WS₂ Nanoparticles Under Mixed Lubrication, *Wear*, 2003, **255**, p 785–793
18. US Patent No. 1714565 (1927) to W. Koehler, US Patent No. 2156803 (1934) to H.S. Cooper and V.R. Damuet, US Patent No. 2284785 (1939) to J.E. Wikey
19. W.O. Winer, Molybdenum Disulfide as a Lubricant: A Review of the Fundamental Knowledge, *Wear*, 1967, **10**, p 422–452
20. A.A. Elsharkawy, Effects of Lubricant Additives on the Performance of Hydrodynamically Lubricated Journal Bearings, *Tribol. Lett.*, 2005, **18**, p 63–73
21. R.B. Rastogi and M. Yadav, Suspension of Molybdenum–Sulphur Complexes in Paraffin Oil as Extreme Pressure Lubricants, *Tribol. Int.*, 2003, **36**, p 511–516
22. T. Hisakado, T. Tsukizoe, and H. Yoshikawa, Lubrication Mechanism of Solid Lubricants in Oils, *Trans. ASME J. Lubr. Technol.*, 1983, **105**, p 245–253
23. B.K. Prasad, Sliding Wear Characteristics of a Gray Cast Iron as Influenced by the Sliding Speed, Load and Environment, *Tribol. Mater. Surf. Interfaces*, 2008, **2**, p 128–138
24. B.K. Prasad, Sliding wear behaviour of a cast iron as affected by test environment and applied load, *Ind. Lubri. Tribol.*, 2009, **61**, p 161–172
25. B.K. Prasad, Influence of Suspended Talc Particles in Oil and Nature of Material Microconstituents on Sliding Wear Characteristics of Cast Iron and Zinc-Based Alloy, *Can. Metall. Q.*, 2009, **48**, p 455–464
26. B.K. Prasad, Sliding Wear Response of Cast Iron as Influenced by Microstructural Features and Test Condition, *Mater. Sci. Eng. A*, 2007, **456A**, p 373–385
27. B.K. Prasad, Sliding Wear Response of Spheroidal Graphite Cast Iron as Influenced by Applied Pressure, Sliding Speed and Test Environment, *Can. Metall. Q.*, 2008, **47**, p 495–507
28. B.K. Prasad, Sliding Wear Response of a Cast Iron Under Varying Test Environments and Traversal Speed and Pressure Conditions, *Wear*, 2006, **260**, p 1333–1341
29. P.K.D. Poddar and M. Chaudhuri, Chapter 2, Natural Minerals, *Handbook of Ceramics*, S. Kumar, Ed., Kumar and Associates Publishers, Calcutta, 1994, p 53–104
30. Wikipedia, The Free Encyclopedia, Graphite, <http://en.wikipedia.org>
31. P.J. Bryant, P.L. Gutshall, and L.H. Taylor, A Study of Mechanisms of Graphite Friction and Wear, *Wear*, 1964, **7**, p 118–126
32. R.H. Savage, Graphite Lubrication, *J. Appl. Phys.*, 1948, **19**, p 1–10
33. H.E. Sliney, Solid Lubricants, *Metals Handbook: Friction, Lubrication, Wear Technology*, Vol. 10, 18th ed., ASM, Materials Park, Ohio, USA, 1992, p 113–122
34. Y. Lakhtin, Chapter 1, Crystal Structure of Metals, *Engineering Physical Metallurgy*, 1st ed., Mir Publishers, Moscow, 1963, p 11–24
35. A.F. Wells, *Structural Inorganic Chemistry*, Clarendon Press, Oxford, 1984
36. T. Bartels, *Lubricants and Lubrication*, *Ullman's Encyclopedia of Industrial Chemistry*, Wiley VCH, Weinheim, 2002
37. P.K. Rohatgi, R. Asthana, and S. Das, Solidification, Structures, and Properties of Cast Metal-Ceramic Particle Composites, *Int. Met. Rev.*, 1986, **31**, p 115–139
38. P.K. Rohatgi, S. Ray, and Y. Liu, Tribological Properties of Metal Matrix-Graphite Particle Composites, *Int. Mater. Rev.*, 1992, **37**, p 129–152
39. G. Rowe, Some Observations on the Frictional Behaviour of Boron Nitride and of Graphite, *Wear*, 1960, **3**, p 274–285
40. B.S. Mazumdar, A.H. Yegneswaran, and P.K. Rohatgi, Strength and Fracture Behaviour of Metal Matrix Particulate Composites, *Mater. Sci. Eng.*, 1984, **68**, p 85–96
41. B.K. Prasad and S. Das, The Significance of Matrix Microstructure on the Solid Lubrication Characteristics of Graphite in Aluminium Alloys, *Mater. Sci. Eng. A*, 1991, **144A**, p 229–235
42. B.K. Prasad, A.K. Patwardhan, and A.H. Yegneswaran, Microstructure and Property Characterization of a Modified Zinc-Based Alloy and Comparison with Bearing Alloys, *J. Mater. Eng. Perform.*, 1998, **7**, p 130–135
43. B.K. Prasad, A.K. Patwardhan, and A.H. Yegneswaran, Factors Controlling the Dry Sliding Wear Behaviour of a Lead-Tin Bronze, *Mater. Sci. Technol.*, 1996, **12**, p 427–435
44. S. Das, S.V. Prasad, and T.R. Ramachandran, Tribology of Al–Si Alloy-Graphite Composites: Triboinduced Graphite Films and the Role of Silicon Morphology, *Mater. Sci. Eng. A*, 1991, **138A**, p 123–132
45. B.K. Prasad, A.K. Patwardhan, and A.H. Yegneswaran, Wear Characteristics of a Zinc-Based Alloy Compared with a Conventional Bearing Bronze Under Mixed Lubrication Condition: Effects of Material and Test Parameters, *Can. Met. Q.*, 2001, **40**, p 193–210
46. M.H. Cho, S.J. Kim, R.H. Basch, J.W. Fash, and H. Jang, Tribological Study of Gray Cast Iron with Automotive Brake Linings: The Effect of Rotor Microstructure, *Tribol. Int.*, 2003, **36**, p 537–545
47. A. Rac, Influence of Load and Speed on Wear Characteristics of Grey Cast Iron in Dry Sliding—Selection for Minimum Wear, *Tribol. Int.*, 1985, **18**, p 29–33
48. E. Takeuchi, The Mechanism of Wear of Spheroidal Graphite Cast Iron in Dry Sliding, *Wear*, 1972, **19**, p 267–276
49. E. Takeuchi, The Mechanisms of Wear of Cast Iron in Dry Sliding, *Wear*, 1968, **11**, p 201–212
50. R.S. Montgomery, The Mild Wear Mechanism of Nodular Iron, *Wear*, 1969, **13**, p 337–343
51. Y.S. Lerner, Wear Resistance of Ductile Irons, *J. Mater. Eng. Perform.*, 1994, **3**, p 403–408
52. L. Fang, Y. Gao, L. Zhou, and P. Li, Unlubricated Sliding Wear of Ceramics Against Graphitized Cast Irons, *Wear*, 1994, **171**, p 129–134
53. F. Wilson and T.S. Eyre, Effect of Matrix Structure and Hardness on the Wear Characteristics of an S.G. Cast Iron, *Wear*, 1969, **14**, p 107–117
54. J.H. Zhu, P.K. Liaw, J.M. Corum, J.G.R. Hansen, and J.A. Cornie, Damage Mechanisms in a Cast Ductile Iron and a Al₂O₃/Al Composite, *Metall. Mater. Trans. A*, 1998, **29A**, p 2855–2862
55. A.K. Jha, B.K. Prasad, O.P. Modi, S. Das, and A.H. Yegneswaran, Correlating Microstructural Features and Mechanical Properties with Abrasion Resistance of a High Strength Low Alloy Steel, *Wear*, 2003, **254**, p 120–128
56. M.V. Rayiko and N.F. Dmytrychenko, Some Aspects of Boundary Lubrication in the Local Contact of Friction Surfaces, *Wear*, 1988, **126**, p 69–78
57. O.P. Modi, B.K. Prasad, A.H. Yegneswaran, and M.L. Vaidya, Dry Sliding Wear Behaviour of Squeeze Cast Aluminium Alloy-Silicon Carbide Composites, *Mater. Sci. Eng. A*, 1992, **151A**, p 235–245
58. F.E. Kennedy, Jr., Thermal and Thermomechanical Effects in Dry Sliding, *Wear*, 1984, **100**, p 453–476
59. L.H. Chen and D.A. Rigney, Transfer During Unlubricated Sliding Wear of Selected Metal Systems, *Wear*, 1985, **105**, p 47–61
60. D.A. Rigney, L.H. Chen, M.G.S. Naylor, and A.R. Rosenfield, Wear Processes in Sliding Systems, *Wear*, 1984, **100**, p 195–219
61. B.K. Prasad and S.V. Prasad, Microstructural Changes During Low-Stress Abrasion of a Plain Carbon (0.5% C) Steel, *Wear*, 1991, **151**, p 1–12
62. B.R. Newcomb and W.M. Stobbs, A Transmission Electron Microscopy Study of the White Etching Layer on a Rail Head, *Mater. Sci. Eng.*, 1984, **66**, p 195–204
63. J. Larsen-Badse and K.G. Mathew, Influence of Structure on the Abrasion Resistance of 1040 Steel, *Wear*, 1969, **14**, p 199–205